BAYESIAN JOINT ESTIMATION OF THE MULTIFRACTALITY PARAMETER OF IMAGE PATCHES USING GAMMA MARKOV RANDOM FIELD PRIORS

S. Combrexelle[1]*, H. Wendt*[1]*, Y. Altmann*[2]*, J.-Y. Tourneret*[1]*, S. McLaughlin*[2]*, P. Abry*[3]

[1] IRIT - ENSEEIHT, CNRS, Univ. of Toulouse, F-31062 Toulouse, France, firstname.lastname@enseeiht.fr

[2] School of Engineering and Physical Sciences, Heriot-Watt Univ., Edinburgh, UK, initial.lastname@hw.ac.uk

[3] CNRS, Physics Dept., Ecole Normale Supérieure de Lyon, F-69364 Lyon, France, patrice.abry@ens-lyon.fr

ABSTRACT

Texture analysis can be embedded in the mathematical framework of multifractal (MF) analysis, enabling the study of the fluctuations in regularity of image intensity and providing practical tools for their assessment, wavelet leaders. A statistical model for leaders was proposed permitting Bayesian estimation of MF parameters for images yielding improved estimation quality over linear regression based estimation. This present work proposes an extension of this Bayesian model for patch-wise MF analysis of images. Classical MF analysis assumes space homogeneity of the MF properties whereas here we assume MF properties may change between texture elements and we do not know where the changes are located. This paper proposes a joint Bayesian model for patches formulated using spatially smoothing gamma Markov Random Field priors to counterbalance the increased statistical variability of estimates caused by small patch sizes. Numerical simulations based on synthetic multifractal images demonstrate that the proposed algorithm outperforms previous formulations and standard estimators.

***Index Terms*—** Multifractal Analysis, Wavelet Leaders, Bayesian Estimation, Texture Analysis, Gamma Markov Random Field

1. INTRODUCTION

Context. Texture analysis is an important field in image processing conducted using various paradigms [1]. Among them, the mathematical framework of multifractal analysis has recently proven to be particularly relevant, cf., e.g., [2, 3] and references therein. Multifractal analysis describes the image texture in terms of the spatial fluctuations of the degree of smoothness of the image intensity at each point. More precisely, the texture of an image $\boldsymbol{X}$ is quantified by means of the *multifractal spectrum* $D(h)$, which is defined as the Hausdorff dimension of the sets of points that possess the same pointwise Hölder regularity h, cf., e.g., [4–7].

Multifractal models are specific instances of scale invariant models and can be practically assessed by studying, over a range of scales 2^j, the power law behaviors of the sample moments of suitably designed multiresolution quantities $T_{\boldsymbol{X}}(j,\boldsymbol{k})$ of $\boldsymbol{X}$ (i.e., quantities that depend jointly on scale 2^j and spatial position $\boldsymbol{k}$)

$$S(q,j) \triangleq \frac{1}{n_j}\sum_{\boldsymbol{k}} |T_{\boldsymbol{X}}(j,\boldsymbol{k})|^q \simeq (2^j)^{\zeta(q)},\ j_1 \le j \le j_2 \quad (1)$$

where $n_j = \mathrm{card}(T_{\boldsymbol{X}}(j,\cdot))$ is the number of $T_{\boldsymbol{X}}(j,\boldsymbol{k})$ at scale j. The multiresolution quantities used in this work are the *wavelet leaders* $l(j,\boldsymbol{k})$ (defined in Section 2), which can be shown to be specifically appropriate for multifractal analysis purposes [2, 5].

The *scaling exponents* $\zeta(q)$ characterizing the power law behavior in (1) are intimately tied to the multifractal spectrum of the image by a Legendre transform, $D(h) \le \mathcal{L}(h) \triangleq \inf_{q\in\mathbb{R}}[2+qh-\zeta(q)]$, and this link enables the practical assessment of multifractal models. Specifically, it permits discrimination between the two most important classes of models: Self-similar models [8], which translate into a strictly linear behavior of $\zeta(q)$ in the neighborhood of $q=0$; Multifractal multiplicative cascade (MMC) based processes [9] which yield a strictly concave function $\zeta(q)$. This difference can be quantified by considering the coefficients of a polynomial development of $\zeta(q)$ at the origin, $\zeta(q) = \sum_{m\ge1} c_m q^m/m!$ [2, 10, 11]. In particular, it can be shown that the second coefficient c_2, called the *multifractality parameter*, is identically zero for self-similar processes but strictly negative for MMC [5, 11]. It therefore enables us to decide which model is better adapted to data in applications, which renders its estimation a central element in multifractal analysis. The reader is referred to, e.g., [4–7], for further details on multifractal analysis.

Estimation of c_2 for image patches. The multifractality parameter c_2 can be shown to be directly linked to the variance of the logarithm of the multiresolution quantities [10]

$$C_2(j) \triangleq \mathrm{Var}\,[\ln l(j,\boldsymbol{k})] = c_2^0 + c_2 \ln 2^j. \quad (2)$$

This leads to the definition of the standard estimation procedure for c_2 as a linear regression of the sample variance $\widehat{\mathrm{Var}}\,[\cdot]$ of the log-leaders with respect to scale j

$$\hat{c}_2 = \frac{1}{\ln 2}\sum_{j=j_1}^{j_2} w_j\, \widehat{\mathrm{Var}}\,[\ln l(j,\cdot)] \quad (3)$$

where w_j are appropriate regression weights [2, 12, 13]. While the simplicity of (3) is attractive, the estimator is known to yield poor performance (large variance) even for moderate image size, which strongly limits its relevance for the analysis of image patches.

An attempt to improve estimation performance was described in [14], which introduced an estimator based on the generalized method of moments. However, this estimator relies on fully parametric models that are too restrictive for real-world images. More recently, Bayesian estimators of c_2 have been investigated for images of relatively small sizes [3, 15]. At the core of this approach is a generic semi-parametric model for the statistics of the log-leaders whose variance-covariance structure is controlled by c_2. This model leads to a likelihood that can be efficiently evaluated with a closed-form Whittle approximation. The Bayesian inference was achieved by a Markov chain Monte Carlo (MCMC) algorithm with a Metropolis-Hastings within Gibbs (MHG) sampler. In [16], an alternative data-augmented formulation for the Bayesian model was proposed which

This work was supported by ANR BLANC 2011 AMATIS BS0101102.

S. Combrexelle was supported by the Direction Générale de l'Armement (DGA).

SML acknowledges the support of EPSRC via grant EP/J015180/1.

complies with the use of conjugate priors, hence yielding a more efficient algorithm. While the method significantly improves estimation performance over (3), the variance of estimates for image patches is still too large for practical applications.

Goals and contributions. The goal of this paper is to devise a Bayesian procedure for the joint estimation of c_2 for image patches which further improves the estimation performance of the Bayesian estimator introduced in [16] by exploiting the spatial dependence between patches through appropriate priors, while inheriting the favorable computational cost of [16]. Starting from the statistical model for a single image introduced in [3, 15, 16] (recalled in Section 2), the proposed procedure relies on the following original key ingredients (detailed in Section 3). First, the joint likelihood of all image patches is expressed as the product of the augmented likelihood of each individual patch given by [16]. Then, a hidden gamma Markov random field (GMRF) [17] with four-fold spatial neighborhood is assigned as a joint prior for the multifractality parameters of the image patches. It relies on the use of a set of auxiliary variables that model positive dependence between the parameters of neighboring image patches. The GMRF prior and data augmentation scheme are designed in such a way that the conditional distributions of the resulting joint posterior can be sampled directly (and thus efficiently), without the need of Metropolis-Hastings steps. The computation of the Bayesian estimator associated with the proposed model is performed by means of an MCMC algorithm, which samples an appropriate target distribution resulting from the data augmentation procedure to then approximate Bayesian estimators of the variables of interest.

The performance of the joint estimation procedure of parameters c_2 associated with image patches is studied in Section 4 by numerical simulations conducted with synthetic multifractal images. These images have prescribed piece-wise homogeneous multifractal properties yielding a controlled ground truth. The proposed method significantly outperforms the linear regression (3), reducing root mean squared error (RMSE) values by one order of magnitude, as well as the Bayesian estimators in [3, 15, 16]. It enables, for the first time, the reliable assessment of small local changes in c_2 between image patches.

2. STATISTICAL MODEL FOR LOG-LEADERS

2.1. Time-domain statistical model

Wavelet leaders. 2D wavelets are commonly defined as tensorial products of the scaling function $\phi(x)$ and mother wavelet $\psi(x)$ of a 1D multiresolution analysis, $\psi^{(0)}(\mathbf{x}) = \phi(x_1)\phi(x_2)$, $\psi^{(1)}(\mathbf{x}) = \psi(x_1)\phi(x_2)$, $\psi^{(2)}(\mathbf{x}) = \phi(x_1)\psi(x_2)$, $\psi^{(3)}(\mathbf{x}) = \psi(x_1)\psi(x_2)$ [18, 19]. When ψ is suitably chosen, the dilated and translated templates denoted $\psi^{(m)}_{j,k}(\mathbf{x}) = 2^{-j/2}\psi^{(m)}(2^{-j}\mathbf{x} - \boldsymbol{k})$ $\psi^{(m)}$, where $a = 2^j$ and $\mathbf{x} = 2^j\boldsymbol{k}$, $\boldsymbol{k} = (k_1, k_2)$, form a basis of $L^2(\mathbb{R}^2)$. The L^1 normalized discrete wavelet transform coefficients of an image $\boldsymbol{X}$ are defined as $d^{(m)}_X(j,k) = \langle \boldsymbol{X}, 2^{-j/2}\psi^{(m)}_{j,k}\rangle$, $m = 0, \ldots, 3$ [18].

Let $\lambda_{j,\boldsymbol{k}}$ denote the dyadic cube of side length 2^j centred at $\boldsymbol{k}2^j$ and $3\lambda_{j,\boldsymbol{k}} = \bigcup_{n_1,n_2=\{-1,0,1\}} \lambda_{j,k_1+n_1,k_2+n_2}$ the union with its eight neighbors. The wavelet leaders are defined as the supremum of the wavelet coefficients within $3\lambda_{j,\boldsymbol{k}}$ over all finer scales [2, 5], i.e.,

$$l(j,\boldsymbol{k}) \triangleq \sup_{m\in(1,2,3),\lambda'\subset 3\lambda_{j,\boldsymbol{k}}} |d^{(m)}_X(\lambda')|. \tag{4}$$

Statistical model. We denote by $\boldsymbol{\ell}_j$ the vector of all log-leaders $\ell(j,\cdot) \triangleq \ln l(j,\cdot)$ at scale j after mean subtraction (the mean does not convey any information on c_2). It has recently been shown that for MMC based processes, the statistics of $\boldsymbol{\ell}_j$ can be well approximated by a multivariate Gaussian distribution whose covariance $\mathcal{C}_j(\boldsymbol{k}, \boldsymbol{\Delta k}) \triangleq \mathrm{Cov}[\ell(j,\boldsymbol{k}), \ell(j,\boldsymbol{k}+\boldsymbol{\Delta k})]$ is modeled by a radial symmetric function parametrized only by $\boldsymbol{\theta} = (c_2, c_2^0)$

$$\mathcal{C}_j(\boldsymbol{k},\boldsymbol{\Delta k}) \approx \varrho_j(||\boldsymbol{\Delta k}||;\boldsymbol{\theta}) \triangleq \begin{cases} \varrho^0_j(||\boldsymbol{\Delta k}||;\boldsymbol{\theta}) & ||\boldsymbol{\Delta k}|| \le 3 \\ \varrho^1_j(||\boldsymbol{\Delta k}||;\boldsymbol{\theta}) & 3 < ||\boldsymbol{\Delta k}|| \end{cases} \tag{5}$$

where $||\cdot||$ is the Euclidian norm, $\varrho^0_j(r;\boldsymbol{\theta}) \triangleq a_j \ln(1+r) + c_2^0 + c_2 \ln 2^j$ with $a_j \triangleq (\varrho^1_j(3;\boldsymbol{\theta}) - c_2^0 - c_2 \ln 2^j)/\ln 4$, $\varrho^1_j(r;\boldsymbol{\theta}) \triangleq c_2 \ln(4r/\sqrt{n_j})\mathbb{I}_{[0,\sqrt{n_j}/4]}(r)$, $\mathbb{I}_A$ is the indicator function of the set A, cf., [3]. Under these assumptions, the likelihood of $\boldsymbol{\ell}_j$ is given by

$$p(\boldsymbol{\ell}_j|\boldsymbol{\theta}) \propto |\boldsymbol{\Sigma}_{j,\boldsymbol{\theta}}|^{-\frac{1}{2}} \exp\Big(-\frac{1}{2}\boldsymbol{\ell}_j^T \boldsymbol{\Sigma}^{-1}_{j,\boldsymbol{\theta}} \boldsymbol{\ell}_j\Big) \tag{6}$$

where the covariance matrix $\boldsymbol{\Sigma}_{j,\boldsymbol{\theta}}$ is defined by $\varrho_j(||\boldsymbol{\Delta k}||;\boldsymbol{\theta})$, $|\cdot|$ is denoting the determinant and ^{T} the transpose operator.

Whittle approximation. The evaluation of the above likelihood is problematic even for small images since it requires computing the matrix inverse $\boldsymbol{\Sigma}^{-1}_{j,\boldsymbol{\theta}}$. Thus, it has been proposed in [3, 15] to approximate (6) with the asymptotic Whittle likelihood [20–24]

$$p_W(\boldsymbol{\ell}_j|\boldsymbol{\theta}) = \exp\left(-\sum_{\mathbf{m}\in\underline{J}_j} \ln\phi_j(\mathbf{m};\boldsymbol{\theta}) + \frac{\boldsymbol{y}_j^*(\mathbf{m})\boldsymbol{y}_j(\mathbf{m})}{\phi_j(\mathbf{m};\boldsymbol{\theta})}\right). \tag{7}$$

Here, $\mathbf{m}$ are the indices of the frequencies $\boldsymbol{\omega}_{\mathbf{m}} = 2\pi\mathbf{m}/\sqrt{n_j}$ of the discrete Fourier transform for one Fourier half-plane[1] $\underline{J}_j$, $\boldsymbol{y}_j \triangleq \mathcal{F}(\boldsymbol{\ell}_j)$ where the operator $\mathcal{F}(\cdot)$ computes and vectorizes the discrete Fourier transform coefficients contained in $\underline{J}_j$ and * stands for complex conjugation. The function $\phi_j(\mathbf{m};\boldsymbol{\theta})$ corresponds to the discretized parametric spectral density associated with the model (5) and has a closed-form parametric expression given by $\phi_j(\mathbf{m};\boldsymbol{\theta}) = c_2 f_j(\mathbf{m}) + c_2^0 g_j(\mathbf{m})$, where f_j and g_j do not depend on $\boldsymbol{\theta}$ and can be precomputed and stored in two vectors denoted as $\mathbf{f}_j \triangleq (f_j(\mathbf{m}))_{\mathbf{m}\in\underline{J}_j}$ and $\mathbf{g}_j \triangleq (g_j(\mathbf{m}))_{\mathbf{m}\in\underline{J}_j}$, see [15] for details. Furthermore, independence is assumed between different scales j, which leads to the following Whittle likelihood for all log-leaders $\boldsymbol{\ell} \triangleq [\boldsymbol{\ell}_{j_1}^T, \ldots, \boldsymbol{\ell}_{j_2}^T]^T$

$$p_W(\boldsymbol{\ell}|\boldsymbol{\theta}) = \prod_{j=j_1}^{j_2} p_W(\boldsymbol{\ell}_j|\boldsymbol{\theta}). \tag{8}$$

2.2. Data augmented statistical model in the Fourier domain

The parameters $\boldsymbol{\theta}$ are encoded implicitly in $\boldsymbol{\Sigma}^{-1}_{j,\boldsymbol{\theta}}$, and their conditional distributions are thus not standard. Sampling the posterior distribution with an MCMC method would thus require accept/reject procedures, such as MHG moves [3]. To obtain a more efficient algorithm, (8) can be interpreted as a statistical model for the Fourier coefficients $\boldsymbol{y}_j$ [16]. More precisely, (8) can be rewritten as

$$p_W(\boldsymbol{\ell}|\boldsymbol{\theta}) = |\boldsymbol{\Gamma}_{\boldsymbol{\theta}}|^{-1} \exp\left(-\boldsymbol{y}^H \boldsymbol{\Gamma}_{\boldsymbol{\theta}}^{-1} \boldsymbol{y}\right), \tag{9}$$
$$\boldsymbol{y} \triangleq [\boldsymbol{y}_{j_1}^T, ..., \boldsymbol{y}_{j_2}^T]^T, \quad \boldsymbol{y}_j = \mathcal{F}(\boldsymbol{\ell}_j)$$

where ^{H} is the conjugate transpose operator and the $N_Y \times N_Y$ diagonal covariance matrix $\boldsymbol{\Gamma}_{\boldsymbol{\theta}}$, with $N_Y \triangleq \mathrm{card}(\boldsymbol{y})$, is given by $\boldsymbol{\Gamma}_{\boldsymbol{\theta}} \triangleq$

[1] Note that due to properties of Fourier transform of real functions, only half of the frequency plane needs to be considered in (7).

$c_2\boldsymbol{F}+c_2^0\boldsymbol{G}$ with $\boldsymbol{F}\triangleq\text{diag}\,(\mathbf{f})$, $\boldsymbol{G}\triangleq\text{diag}\,(\mathbf{g})$, $\mathbf{f}\triangleq[\mathbf{f}_{j_1}^T,...,\mathbf{f}_{j_2}^T]^T$ and $\mathbf{g}\triangleq[\mathbf{g}_{j_1}^T,...,\mathbf{g}_{j_2}^T]^T$. Assuming that $\boldsymbol{\Gamma}_{\boldsymbol{\theta}}$ is positive definite, (9) amounts to modeling the Fourier coefficients $\boldsymbol{y}$ by a random vector with a centered circular-symmetric complex Gaussian distribution $\mathcal{CN}(\mathbf{0},\boldsymbol{\Gamma}_{\boldsymbol{\theta}})$ [25], hence to the use of the likelihood

$$p(\boldsymbol{y}|\boldsymbol{\theta})=|\boldsymbol{\Gamma}_{\boldsymbol{\theta}}|^{-1}\exp\left(-\boldsymbol{y}^H\boldsymbol{\Gamma}_{\boldsymbol{\theta}}^{-1}\boldsymbol{y}\right). \tag{10}$$

Reparametrization. The matrix $\boldsymbol{\Gamma}_{\boldsymbol{\theta}}$ is positive definite as long as the parameters $\boldsymbol{\theta}=(c_2,c_2^0)$ belong to the admissible set

$$\mathcal{A}=\{\boldsymbol{\theta}\in\mathbb{R}_\star^-\times\mathbb{R}_\star^+|c_2\mathbf{f}(k)+c_2^0\mathbf{g}(k)>0,k=1,\ldots,N_Y\}. \tag{11}$$

It can be shown that $\forall k, c_2^0\mathbf{g}(k)>0$ (while $\exists k|\mathbf{f}(k)<0$) [15] and hence that (11) can be transformed into independent positivity constraints after reparametrization by the mapping $\boldsymbol{\theta}\mapsto\boldsymbol{v}\triangleq(-c_2,c_2^0/\gamma+c_2)$, where $\gamma=\sup_k\mathbf{f}(k)/\mathbf{g}(k)$ [16]. This map defines a one-to-one transformation from $\boldsymbol{\theta}\in\mathcal{A}$ to $\boldsymbol{v}\in\mathbb{R}_\star^{+2}$ and (10) can be expressed with $\boldsymbol{v}$ as

$$\begin{aligned}p(\boldsymbol{y}|\boldsymbol{v})\propto&|\boldsymbol{\Gamma}_{\boldsymbol{v}}|^{-1}\exp\left(-\boldsymbol{y}^H\boldsymbol{\Gamma}_{\boldsymbol{v}}^{-1}\boldsymbol{y}\right)\\ &\boldsymbol{\Gamma}_{\boldsymbol{v}}=v_1\tilde{\boldsymbol{F}}+v_2\tilde{\boldsymbol{G}},\quad\tilde{\boldsymbol{F}}=-\boldsymbol{F}+\boldsymbol{G}\gamma,\quad\tilde{\boldsymbol{G}}=\boldsymbol{G}\gamma.\end{aligned} \tag{12}$$

where the diagonal matrices $\tilde{\boldsymbol{F}}$, $\tilde{\boldsymbol{G}}$ and $\boldsymbol{\Gamma}_{\boldsymbol{v}}$, for $\boldsymbol{v}\in\mathbb{R}_\star^{+2}$, are by construction positive definite.

Data augmentation. The likelihood (12) is finally extended using the model $\boldsymbol{y}|\boldsymbol{\mu},v_2\sim\mathcal{CN}(\boldsymbol{\mu},v_2\tilde{\boldsymbol{G}})$, $\boldsymbol{\mu}|v_1\sim\mathcal{CN}(0,v_1\tilde{\boldsymbol{F}})$, where $\boldsymbol{\mu}$ is an $N_Y\times1$ vector of additional latent variables [16]. This model is associated with the extended likelihood

$$\begin{aligned}p(\boldsymbol{y},\boldsymbol{\mu}|\boldsymbol{v})\propto&{v_2}^{-N_Y}\exp\Big(-\frac{1}{v_2}(\boldsymbol{y}-\boldsymbol{\mu})^H\tilde{\boldsymbol{G}}^{-1}(\boldsymbol{y}-\boldsymbol{\mu})\Big)\\ &\times{v_1}^{-N_Y}\exp\Big(-\frac{1}{v_1}\boldsymbol{\mu}^H\tilde{\boldsymbol{F}}^{-1}\boldsymbol{\mu}\Big)\end{aligned} \tag{13}$$

from which (12) can be recovered by marginalization with respect to $\boldsymbol{\mu}$. One easily verifies that (13) leads to standard conditional distributions when inverse-gamma ($\mathcal{IG}$) priors are used for $v_i\in\mathbb{R}_\star^+$.

3. BAYESIAN ESTIMATION FOR IMAGE PATCHES

Based on the likelihood (13) for one single image (or patch), we now formulate our joint Bayesian model for image patches.

3.1. Likelihood

Denote as $\{\boldsymbol{X}_{\boldsymbol{k}}\}$ a partition of the image $\boldsymbol{X}$ into non-overlapping patches $\boldsymbol{X}_{\boldsymbol{k}}$ of size $N\times N$, and as $\boldsymbol{y}_{\boldsymbol{k}}$, $\boldsymbol{\mu}_{\boldsymbol{k}}$ and $\boldsymbol{v}_{\boldsymbol{k}}$ the Fourier coefficients, latent variables and parameter vector associated with patch $\boldsymbol{X}_{\boldsymbol{k}}$. Let furthermore denote $\boldsymbol{Y}\triangleq\{\boldsymbol{y}_{\boldsymbol{k}}\}$, $\boldsymbol{M}\triangleq\{\boldsymbol{\mu}_{\boldsymbol{k}}\}$, and $\boldsymbol{V}\triangleq\{\boldsymbol{V}_1,\boldsymbol{V}_2\}$ with $\boldsymbol{V}_i\triangleq\{v_{i,\boldsymbol{k}}\}$, $i=1,2$. With the assumptions of Section 2, the joint likelihood of $\boldsymbol{Y}$ can be written

$$p(\boldsymbol{Y},\boldsymbol{M}|\boldsymbol{V})\propto\prod_{\boldsymbol{k}}p(\boldsymbol{y}_{\boldsymbol{k}},\boldsymbol{\mu}_{\boldsymbol{k}}|\boldsymbol{v}_{\boldsymbol{k}}). \tag{14}$$

3.2. Gamma Markov random field prior

Inverse-gamma distributions $\mathcal{IG}(\alpha_{i,\boldsymbol{k}},\beta_{i,\boldsymbol{k}})$ are conjugate priors for the parameters $v_{i,\boldsymbol{k}}$ in (14), where $i=1,2$. We propose here to specify $(\alpha_{i,\boldsymbol{k}},\beta_{i,\boldsymbol{k}})$ such that the resulting prior for $\boldsymbol{V}_i$ is a hidden GMRF [17], which relies on the use of a set of positive auxiliary variables $\boldsymbol{Z}=\{\boldsymbol{Z}_1,\boldsymbol{Z}_2\}$, $\boldsymbol{Z}_i=\{z_{i,\boldsymbol{k}}\}$, to induce positive dependence between the neighbooring elements of $\boldsymbol{V}_i$ [17] and hence spatial regularization. More precisely, each $v_{i,\boldsymbol{k}}$ is connected to the four auxiliary variables $z_{i,\boldsymbol{k}'}>0$, $\boldsymbol{k}'\in\mathcal{V}_v(\boldsymbol{k})\triangleq\{(k_1,k_2),(k_1+1,k_2),(k_1,k_2+1),(k_1+1,k_2+1)\}$ (and thus, each $z_{i,\boldsymbol{k}}$ to $v_{i,\boldsymbol{k}'}$, $\boldsymbol{k}'\in\mathcal{V}_z(\boldsymbol{k})=\{(k_1-1,k_2-1),(k_1,k_2-1),(k_1-1,k_2),(k_1,k_2)\}$), via edges weighted by a_i, which act as a regularization parameters controlling the amount of spatial smoothness. This GMRF prior for $(\boldsymbol{V}_i,\boldsymbol{Z}_i)$ can be shown to be associated with the density [17]

$$\begin{aligned}p(\boldsymbol{V}_i,\boldsymbol{Z}_i|a_i)=C(a_i)^{-1}\prod\nolimits_{\boldsymbol{k}}&\,\mathrm{e}^{-(4a_i+1)\log v_{i,\boldsymbol{k}}}\,\mathrm{e}^{(4a_i-1)\log z_{i,\boldsymbol{k}}}\\ &\times\,\mathrm{e}^{-\frac{a_i}{v_{i,\boldsymbol{k}}}\sum_{\boldsymbol{k}'\in\mathcal{V}_v(\boldsymbol{k})}z_{i,\boldsymbol{k}'}}\end{aligned} \tag{15}$$

where $C(a_i)$ is an (intractable) normalization constant.

Posterior. Assuming prior independence between $(\boldsymbol{V}_1,\boldsymbol{Z}_1)$ and $(\boldsymbol{V}_2,\boldsymbol{M},\boldsymbol{Z}_2)$, Bayes' theorem yields the joint posterior distribution associated with the proposed model

$$\begin{aligned}p(\boldsymbol{V},\boldsymbol{Z},\boldsymbol{M}|\boldsymbol{Y},a_1,a_2)\;\propto\;&p(\boldsymbol{Y}|\boldsymbol{V}_2,\boldsymbol{M})\,p(\boldsymbol{M}|\boldsymbol{V}_1)\\ &\times p(\boldsymbol{V}_1,\boldsymbol{Z}_1|a_1)\,p(\boldsymbol{V}_2,\boldsymbol{Z}_2|a_2)\end{aligned} \tag{16}$$

where a_i, $i=1,2$, are fixed hyperparameters.

3.3. Bayesian estimators

Since we are interested in the parameters $\boldsymbol{V}_i$ only, we consider the marginal posterior mean estimator for $\boldsymbol{V}_i$, denoted MMSE (minimum mean square error estimator) and defined as $\boldsymbol{V}_i^{\text{MMSE}}\triangleq\mathbb{E}[\boldsymbol{V}_i|\boldsymbol{Y},a_i]$, where the expectation is taken with respect to the marginal posterior density $p(\boldsymbol{V}_i|\boldsymbol{Y},a_i)$. Note that the direct computation of $\boldsymbol{V}_i^{\text{MMSE}}$ is not tractable as it requires integrating the full posterior (16) over all other unknown variables. By considering a Gibbs sampler (GS) drawing samples $(\{\boldsymbol{V}_i^{(k)}\},\boldsymbol{M}^{(k)},\{\boldsymbol{Z}_i{}^{(k)}\})_{k=1}^{N_{mc}}$ asymptotically distributed according to (16), we can however approximate $\boldsymbol{V}_i^{\text{MMSE}}$ using the samples $\boldsymbol{V}_i^{(k)}$ [26] as

$$\boldsymbol{V}_i^{\text{MMSE}}\approx(N_{mc}-N_{bi})^{-1}\sum\nolimits_{k=N_{bi}}^{N_{mc}}\boldsymbol{V}_i^{(k)} \tag{17}$$

where N_{bi} is the length of the burn-in period.

3.4. Gibbs sampler

The GS consists of successively generating samples from the conditional distributions associated with the target distribution, here the posterior [26]. The conditionals for (16) can be easily calculated

$$\boldsymbol{\mu}_{\boldsymbol{k}}|\boldsymbol{Y},\boldsymbol{V}\sim\mathcal{CN}\Big(v_{1,\boldsymbol{k}}\tilde{\boldsymbol{F}}\boldsymbol{\Gamma}_{\boldsymbol{v}_{\boldsymbol{k}}}^{-1}\boldsymbol{y}_{\boldsymbol{k}},\Big((v_{1,\boldsymbol{k}}\tilde{\boldsymbol{F}})^{-1}+(v_{2,\boldsymbol{k}}\tilde{\boldsymbol{G}})^{-1}\Big)^{-1}\Big) \tag{18a}$$

$$v_{1,\boldsymbol{k}}|\boldsymbol{M},\boldsymbol{Z}_1\sim\mathcal{IG}\big(N_Y+\alpha_{1,\boldsymbol{k}},||\boldsymbol{\mu}_{\boldsymbol{k}}||_{\tilde{\boldsymbol{F}}^{-1}}+\beta_{1,\boldsymbol{k}}\big) \tag{18b}$$

$$v_{2,\boldsymbol{k}}|\boldsymbol{Y},\boldsymbol{M},\boldsymbol{Z}_2\sim\mathcal{IG}\big(N_Y+\alpha_{2,\boldsymbol{k}},||\boldsymbol{y}_{\boldsymbol{k}}-\boldsymbol{\mu}_{\boldsymbol{k}}||_{\tilde{\boldsymbol{G}}^{-1}}+\beta_{2,\boldsymbol{k}}\big) \tag{18c}$$

$$z_{i,\boldsymbol{k}}|\boldsymbol{V}_i\sim\mathcal{G}(\tilde{\alpha}_{i,\boldsymbol{k}},\tilde{\beta}_{i,\boldsymbol{k}}) \tag{18d}$$

where $||\mathbf{x}||_\Pi\triangleq\mathbf{x}^H\Pi\mathbf{x}$, $\alpha_{i,\boldsymbol{k}}=\tilde{\alpha}_{i,\boldsymbol{k}}=4a_i$, $\beta_{i,\boldsymbol{k}}=a_i\sum_{\boldsymbol{k}'\in\mathcal{V}_v(\boldsymbol{k})}z_{i,\boldsymbol{k}'}$ and $\tilde{\beta}_{i,\boldsymbol{k}}=(a_i\sum_{\boldsymbol{k}'\in\mathcal{V}_z(\boldsymbol{k})}v_{i,\boldsymbol{k}'}^{-1})^{-1}$. Note that all conditionals (18a–18d) are standard laws that can be sampled efficiently, without Metropolis-Hastings acceptance-reject steps.

Finally, note that it is easy to show that assuming independence between parameters $v_{i,\boldsymbol{k}}$, that have inverse-gamma priors $\mathcal{IG}(c_i,d_i)$ instead of (15), leads to a Bayesian model that can be sampled using GS steps defined in (18a–18c) with parameters $\alpha_{i,\boldsymbol{k}}=c_i$ and $\beta_{i,\boldsymbol{k}}=d_i$. This model is equivalent to the one studied in [16].

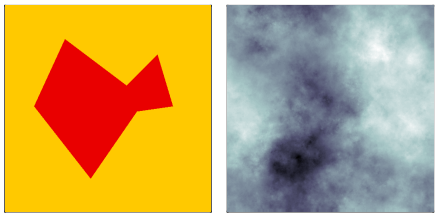

Fig. 1. Mask of piecewise constant values of $c_2 \in \{-0.02, -0.04\}$ (middle); one realization of MRW with the values of c_2 displayed in the middle figure (right).

4. NUMERICAL EXPERIMENTS

The proposed Bayesian estimator for the multifractality parameters associated with image patches (with spatial GMRF prior, denoted GMRF) was applied to independent realizations of 2D multifractal random walks (MRWs) of size 2048×2048, with two distinct zones of homogeneous multifractality. MRWs are MMC processes that have multifractal properties similar to those of Mandelbrot's log-normal cascades, with scaling exponents $\zeta(q) = (H - c_2)q + c_2q^2$ (cf., [27] for details). A typical realization is plotted in Fig. 1 (right) together with the zones of constant multifractality parameter used here (a polygon with $c_2 = -0.04$ and a background with $c_2 = -0.02$). This piece-wise constant spatial evolution of c_2 is chosen here as a limit case test for GMRF (which is actually designed for smooth evolutions). We use non-overlapping patches of size $N \times N = 64 \times 64$ and compare the proposed estimator with its counterpart with $\mathcal{IG}$ prior of [16] (denoted IG) and the standard linear regression based estimator (using (3) with weights w_j as in [2, 12, 13] and denoted as LF). The regularization parameters of GMRF have been fixed to $a_i = 10$ using cross-validation (note that results have been found to be robust with respect to the precise choice of a_i).

Illustration for a single realization. Fig. 2 (top row) shows patch-wise estimates of c_2 obtained with LF, IG and GMRF (from left to right). Clearly, LF fails to reveal the two zones with distinct values of c_2 in the image. The Bayesian estimator IG improves the estimation quality significantly as compared to LF and enables the visual identification of the polygon. Yet, estimates obtained with IG still display strong variability. In contrast, the proposed Bayesian estimator with GMRF prior yields excellent estimates that closely reproduce the prescribed zones with constant c_2. A more quantitative analysis is proposed in Fig. 2 (bottom row), which shows the results of a classification of the patch-wise estimates of c_2, obtained by histogram thresholding using the k-means algorithm with 2 classes. Classification performance is quantified as the percentage of correctly classified pixels in the image and is stated in color in the figure. The results further confirm the above conclusions: LF yields classification performance that is not better than that of random classification; IG enables approximately three quarters of the pixels to be correctly classified; GMRF yields excellent classification results and 95% correctly classified pixels.

Estimation performance. The estimation performance is assessed through the bias, the standard deviation (STD) and the root mean squared error (RMSE) of the different estimators computed for 100 independent realizations and defined by $\mathrm{b} = \widehat{\mathbb{E}}[\hat{c}_2] - c_2$, $\mathrm{s} = (\widehat{\mathrm{Var}}[\hat{c}_2])^{\frac{1}{2}}$ and $\mathrm{rms} = \sqrt{\mathrm{b}^2 + \mathrm{s}^2}$, respectively. Moreover, we compute the average of correctly classified pixels (denoted ccp)

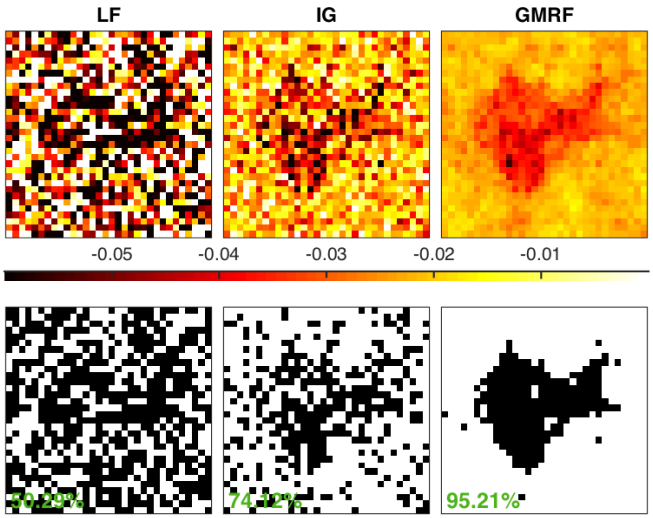

Fig. 2. Patch-wise estimation of c_2 for a single realization of MRW (top; the ground truth and data are plotted in Fig. 1); k-means classification of the estimates (bottom).

for k-means classification of patch-wise estimates as described in the previous paragraph. Results are summarized in Table 1 and strengthen the above conclusions. While the Bayesian estimator IG improves STD and RMSE values by a factor of $3-4$ as compared to LF as reported in [16], the proposed Bayesian estimator GMRF further and significantly improves STD and RMSE values to only $1/10$th of those of LF. The excellent performance of GMRF is also reflected by the classification results: GMRF yields by far the best ccp equal to 94.6%. Finally, note that these performance improvements are achieved at only ≈ 5 times the computational time of LF.

	|b|	s	rms	ccp
LF	0.0055	0.0406	0.0413	54.2
IG	0.0018	0.0123	0.0125	76.5
GMRF	0.0027	0.0032	0.0044	94.6

Table 1. Estimation performance for 100 independent realizations.

5. CONCLUSIONS AND FUTURE PERSPECTIVES

This work investigated a Bayesian model that enables the joint estimation of the multifractality parameters c_2 of image patches. This relied on the use of a recently proposed data augmented Whittle likelihood for log-leaders and on a suitable GMRF joint prior for the multifractality parameters. This prior efficiently counteracts the large statistical variability of estimates when using small patch sizes for the local assessment of c_2. The parameters of this model can be efficiently estimated using an MCMC algorithm. The proposed procedure yields excellent estimation performance, enabling for the first time the reliable assessment of small differences in c_2 between image patches. Future work will include incorporation of the regularization hyperparameters a_i in the Bayesian model, including the possibility to let a_i take different values for different patches, as well as application to remote sensing images.

6. REFERENCES

[1] R. M. Haralick, "Statistical and structural approaches to texture," *Proc. of the IEEE*, vol. 67, no. 5, pp. 786–804, 1979.

[2] H. Wendt, S. G. Roux, S. Jaffard, and P. Abry, "Wavelet leaders and bootstrap for multifractal analysis of images," *Signal Process.*, vol. 89, no. 6, pp. 1100 – 1114, 2009.

[3] S. Combrexelle, H. Wendt, N. Dobigeon, J.-Y. Tourneret, S. McLaughlin, and P. Abry, "Bayesian estimation of the multifractality parameter for image texture using a Whittle approximation," *IEEE T. Image Proces.*, vol. 24, no. 8, pp. 2540–2551, 2015.

[4] R. H. Riedi, "Multifractal processes," in *Theory and applications of long range dependence*, P. Doukhan, G. Oppenheim, and M.S. Taqqu, Eds. 2003, pp. 625–717, Birkhäuser.

[5] S. Jaffard, "Wavelet techniques in multifractal analysis," in *Fractal Geometry and Applications: A Jubilee of Benoît Mandelbrot, Proc. Symp. Pure Math.*, M. Lapidus and M. van Frankenhuijsen, Eds. 2004, vol. 72(2), pp. 91–152, AMS.

[6] J. F. Muzy, E. Bacry, and A. Arneodo, "The multifractal formalism revisited with wavelets," *Int. J. of Bifurcation and Chaos*, vol. 4, pp. 245–302, 1994.

[7] R. Lopes and N. Betrouni, "Fractal and multifractal analysis: A review," *Medical Image Analysis*, vol. 13, pp. 634–649, 2009.

[8] B. B. Mandelbrot and J. W. van Ness, "Fractional Brownian motion, fractional noises and applications," *SIAM Review*, vol. 10, pp. 422–437, 1968.

[9] B. B. Mandelbrot, "A multifractal walk down Wall Street," *Sci. Am.*, vol. 280, no. 2, pp. 70–73, 1999.

[10] B. Castaing, Y. Gagne, and M. Marchand, "Log-similarity for turbulent flows," *Physica D*, vol. 68, no. 3-4, pp. 387–400, 1993.

[11] H. Wendt, S. Jaffard, and P. Abry, "Multifractal analysis of self-similar processes," in *Proc. IEEE Workshop Statistical Signal Process. (SSP)*, Ann Arbor, USA, 2012.

[12] H. Wendt, P. Abry, and S. Jaffard, "Bootstrap for empirical multifractal analysis," *IEEE Signal Process. Mag.*, vol. 24, no. 4, pp. 38–48, 2007.

[13] P. Abry, R. Baraniuk, P. Flandrin, R. Riedi, and D. Veitch, "Multiscale nature of network traffic," *IEEE Signal Proc. Mag.*, vol. 19, no. 3, pp. 28–46, 2002.

[14] T. Lux, "Higher dimensional multifractal processes: A GMM approach," *J. Business & Economic Stat.*, vol. 26, pp. 194–210, 2007.

[15] S. Combrexelle, H. Wendt, J.-Y. Tourneret, P. Abry, and S. McLaughlin, "Bayesian estimation of the multifractality parameter for images via a closed-form Whittle likelihood," in *Proc. 23rd European Signal Process. Conf. (EUSIPCO)*, Nice, France, 2015.

[16] S. Combrexelle, H. Wendt, Y. Altmann, J.-Y. Tourneret, S. McLaughlin, and P. Abry, "A Bayesian framework for the multifractal analysis of images using data augmentation and a Whittle approximation," in *Proc. IEEE Int. Conf. Acoust., Speech, and Signal Process. (ICASSP)*, Shanghai, China, March 2016.

[17] O. Dikmen and A.T. Cemgil, "Gamma markov random fields for audio source modeling," *IEEE Trans. Audio, Speech, and Language Process.*, vol. 18, no. 3, pp. 589–601, 2010.

[18] S. Mallat, *A Wavelet Tour of Signal Processing*, Academic Press, 3rd edition, 2008.

[19] J.-P. Antoine, R. Murenzi, P. Vandergheynst, and S. T. Ali, *Two-Dimensional Wavelets and their Relatives*, Cambridge University Press, 2004.

[20] P. Whittle, "On stationary processes in the plane," *Biometrika*, vol. 41, pp. 434–449, 1954.

[21] M. Fuentese, "Approximate likelihood for large irregularly spaced spatial data," *J. Am. Statist. Assoc.*, vol. 102, pp. 321–331, 2007.

[22] J. Beran, *Statistics for Long-Memory Processes*, vol. 61 of *Monographs on Statistics and Applied Probability*, Chapman & Hall, New York, 1994.

[23] V. V. Anh and K. E. Lunney, "Parameter estimation of random fields with long-range dependence," *Math. Comput. Model.*, vol. 21, no. 9, pp. 67–77, 1995.

[24] T. S. Rao and R. E. Chandler, "A frequency domain approach for estimating parameters in point process models," in *Proc. Athens Conf. Applied Probability and Time Series Analysis*. Springer, 1996, pp. 392–405.

[25] N. R. Goodman, "Statistical analysis based on a certain multivariate complex gaussian distribution (an introduction)," *Ann. Math. Stat.*, vol. 34, no. 1, pp. pp. 152–177, 1963.

[26] C. P. Robert and G. Casella, *Monte Carlo Statistical Methods*, Springer, New York, USA, 2005.

[27] R. Robert and V. Vargas, "Gaussian multiplicative chaos revisited," *Ann. Proba.*, vol. 38, no. 2, pp. 605–631, 2010.